A Data-Driven Design Framework for Structural Optimization to Enhance Wearing Adaptability of Prosthetic Hands

Yu Gu, Long He, Haozhou Zeng, Jiaxing Li, Ning Zhang, Xiufeng Zhang, and Tao Liu, *Senior Member, IEEE*

***Abstract*— Prosthetic hands have significant potential to restore the manipulative capabilities and self-confidence of amputees and enhance their quality of life. However, incompatibility between prosthetic devices and residual limbs can lead to secondary injuries such as skin pressure ulcers and restricted joint motion, contributing to a high prosthesis abandonment rate. To address these challenges, this study introduces a data-driven design framework (D3Frame) utilizing a multi-index optimization method. By incorporating motion/ pressure data, as well as clinical criteria such as pain threshold/ tolerance, from various anatomical sites on the residual limbs of amputees, this framework aims to optimize the structural design of the prosthetic socket, including the Antecubital Channel (AC), Lateral Epicondylar Region Contour (LC), Medial Epicondylar Region Contour (MC), Olecranon Region Contour (OC), Lateral Flexor/ Extensor Region (LR), and Medial Flexor/ Extensor Region (MR). Experiments on five forearm amputees verified the improved adaptability of the optimized socket compared to traditional sockets under three load conditions. The experimental results revealed a modest score enhancement on standard clinical scales and reduced muscle fatigue levels. Specifically, the percent effort of muscles and slope value of mean/ median frequency decreased by 19%, 70%, and 99% on average, respectively, and the average values of mean/ median frequency in the motion cycle both increased by approximately 5%. The proposed D3Frame in this study was applied to optimize the structural aspects of designated regions of the prosthetic socket, offering the potential to aid prosthetists in prosthesis design and, consequently, augmenting the adaptability of prosthetic devices.**

***Index Terms*— Data-driven design framework, multi-index fusion, structural optimization, prosthetic hand, adaptability performance.**

I. Introduction

UNTIL 2020, the worldwide population afflicted with limb disabilities was estimated to be around 65 million, with an annual increment of 1.5 million [1]. Within this demographic, approximately 40% were upper limb amputees [1], [2]. The clinical research demonstrates that prosthetic hands can assist amputees in the restoration of self-confidence, the reinstatement of functional abilities, and the enhancement of their quality of life [3], [4]. Notwithstanding the intrinsic advantages of prosthetic devices, a high rate of prosthetic apparatus abandonment persists, with around 35% of instances attributed to secondary injuries in residual limbs [3], [5]. Abandonment reasons encompass issues such as the suboptimal fit of the prosthetic socket, skin pressure ulcers resulting from prolonged periods of compression on the soft tissue of the residual limb, and extended prosthetic design cycles. Currently, there exists a pressing demand for the improvement of adaptability in prosthetic socket, and efforts have been made by amalgamating the design expertise of prosthetists [6], [7], utilizing simulation tools [8], and advancing optimization methodologies [9].

The prosthetic socket has been considered the gold standard [10] for limb amputees and is widely accepted due to its affordability, non-invasive nature, and lower risk of infection and fracture compared to other emerging prosthetic adaptation technologies such as osseointegration (OI) [10], [11]. Notably, clinical studies have revealed that a well-matched interface between amputees and the prosthetic socket could reduce muscle burden and decrease the fatigue experienced by amputees employing prosthetic devices [12], [13], [14]. Consequently, efforts have been made by numerous researchers to optimize prosthetic socket design to enhance the wearing adaptability of prosthetic sockets [15], [16], [17].

Manuscript received 13 November 2023; revised 18 June 2024; accepted 15 July 2024. Date of publication 17 July 2024; date of current version 25 July 2024. This work was supported in part by the National Natural Science Foundation of China under Grant 52175033 and Grant U21A20120, and in part by the Key Research and Development Program of Zhejiang Province under Award 2022C03103 and Award 2021C03051. *(Corresponding authors: Tao Liu; Xiufeng Zhang.)*

This work involved human subjects or animals in its research. Approval of all ethical and experimental procedures and protocols was granted by the Medical Ethics Committee of the School of Medicine, Zhejiang University, under Application No. 2021-039.

Yu Gu, Haozhou Zeng, Jiaxing Li, and Tao Liu are with the State Key Laboratory of Fluid Power and Mechatronic Systems, School of Mechanical Engineering, Zhejiang University, Hangzhou 310027, China (e-mail: yu.gu@zju.edu.cn; 22225063@zju.edu.cn; 12225069@zju.edu.cn; liutao@zju.edu.cn).

Long He is with the Zhiyuan Research Institute, Hangzhou 310024, China (e-mail: helong_zyy@163.com).

Ning Zhang and Xiufeng Zhang are with the National Research Center for Rehabilitation Technical Aids, Beijing 100176, China (e-mail: zhangning@mca.gov.cn; zhangxiufeng@mca.gov.cn).

This article has supplementary downloadable material available at https://doi.org/10.1109/TNSRE.2024.3430070, provided by the authors.

Digital Object Identifier 10.1109/TNSRE.2024.3430070

Early researchers primarily focused on the traditional design method [6], which primarily consisted of casting, modification, and lamination, while the optimization design methods they proposed were largely centered on the selection of anatomical positions and the summarization of design experiences [7]. With the advancement of digital technologies, the focus of researchers has gradually shifted toward 3D printing for upper limb prosthetics [18], motivated by the extended production cycles necessitated by traditional design methods. Additionally, traditional design methods exhibit some shortcomings. The conventional socket fabrication process using plaster of Paris to capture limb shape necessitates the destruction of the plaster model to create the prosthetic socket [19], rendering the plaster molds non-reusable for future applications and offering limited opportunities for correcting errors [12].

Other research has been reported to optimize the design of prosthetic sockets using simulation methods, which primarily involve the utilization of mechanical models and finite element analysis methods [8], [20], [21] to simulate surface pressure information on residual limbs when subjected to external forces. However, given the significant disparity between the simulation results and the actual values, as well as the substantial variations in the mechanical characteristics of the residual limbs among each amputee, such simulation methods were predominantly applied in the assessment of prosthetic socket adaptability [13], [14]. A strategy was subsequently proposed by researchers [9], which integrates the empirically measured mechanical characteristics of residual limbs for simulation and structural optimization, demonstrating favorable outcomes by verification on a lower limb amputee [22].

The current optimization methods in recent research mainly include 1) Numerical simulation, such as the finite-element based method. Due to the spatiotemporal variation characteristics of the residual limb's mechanical properties, using complex mechanical models like viscoelasticity still fails to overcome the significant discrepancies between simulation results and actual values [8], [20]. Thus, the numerical simulation method has limited utility for prosthetic socket structural optimization. 2) single-parameter based optimization methods. For instance, researchers have optimized the design by combining tissue mechanical properties [9] or conducting wear tests based on amputees' subjective feedback [7]. However, the muscle condition and feedback results of amputees exhibit considerable individual differences, making precise and scientific optimization of prosthetic socket structures challenging. Clinical indicators that reflect pain differences, certain physical parameters, and even prosthetists' design experience and guidelines should be integrated into the optimization algorithm to enhance its adaptability to individual differences.

To bridge these gaps mentioned above, a data-driven design framework (D3Frame) centered around a multi-index-based optimization method was presented in this study. This approach incorporated design experience from prosthetists, motion and pressure data derived from specific anatomical sites of amputees, and clinical criteria, such as pain threshold and pain tolerance. Multifaceted information was employed

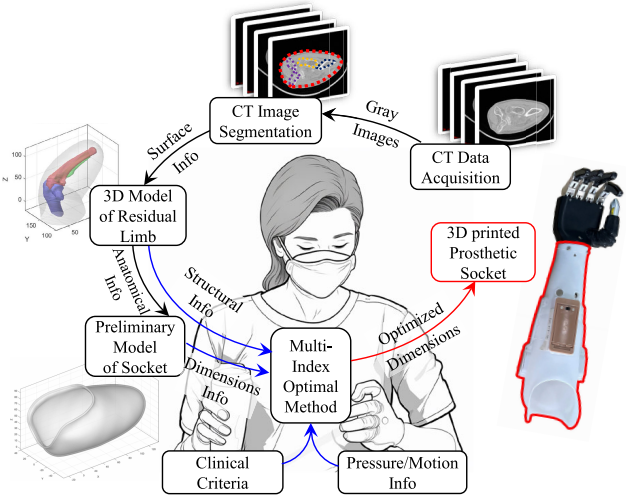

Fig. 1. The proposed design framework includes computed tomography-image based residual limb reconstruction, preliminary socket design, and a multi-index based optimal model for enhancing wearing adaptability in prosthetic hands.

to optimize the compression/expansion size at the selected anatomical positions. Additionally, five forearm amputees were recruited to conduct experiments under three distinct load conditions, compared with the traditional prosthetic socket, to verify the adaptability improvement of the optimized socket in practical applications. The assessment of the capacity for myoelectric control (ACMC) scale and electromyographic (EMG) data were also utilized for the analysis of muscle activation and fatigue levels among subjects using both types of prosthetic sockets. The experimental results further confirmed the adaptability performance of the optimized prosthetic socket for amputees.

Moreover, the paper is organized as follows: Section II provides an introduction to a digital design framework. In Section III, the optimization method is elaborated, encompassing the fusion of multi-indicators extracted from clinical criteria, pressure, and motion information. Section IV presents the experimental protocol and data processing, while Section V presents the results obtained under the three load conditions using two prosthetic socket types. Section VI offers a discussion on the performance of the proposed method in comparison with existing studies. Finally, Section VII concludes the paper.

II. Design Framework

The entire process of the proposed D3Frame for prosthetic socket design is illustrated in Figure 1, including 1) the preliminary design of the prosthetic socket, 2) multi-source information acquisition for optimization, and 3) design optimization based on multi-index information.

A. Preliminary Design of the Prosthetic Socket

1) Residual Limb Reconstruction: Considering the conventional practice of employing plaster of Paris for limb shape capture, which may preclude subsequent optimizations [12], [23], a 3D construction method has been adopted in this study. Diverging from other studies that primarily focus on surface

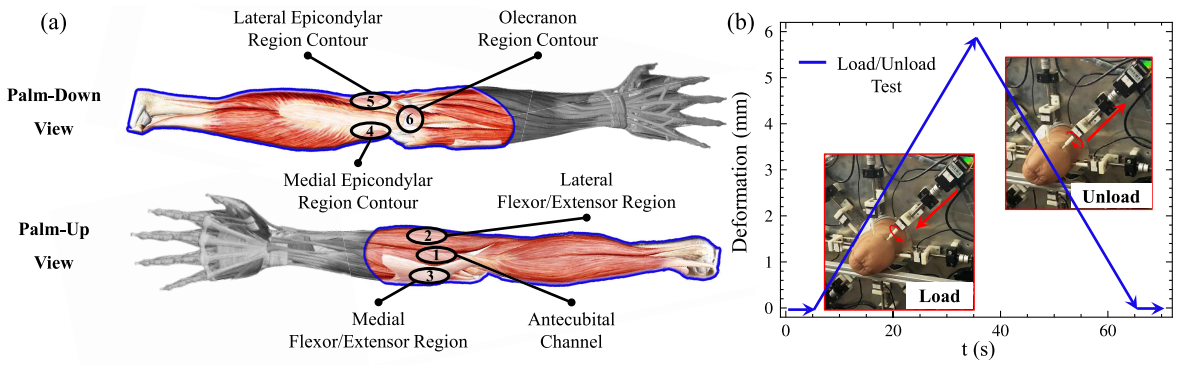

Fig. 2. Measurement regions selected for the indentation test and the force-position loading process. (a) Six anatomical positions were chosen for measuring force-deformation and clinical criteria. (b) The indentation test was conducted at a load/unload speed of 0.2 mm/s.

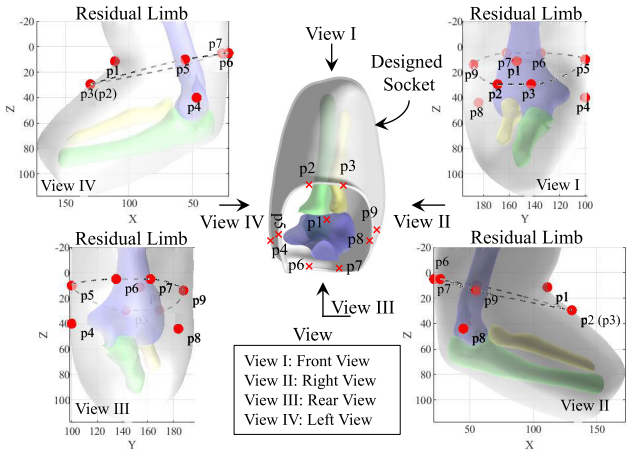

Fig. 3. The preliminary design of a prosthetic socket, demonstrating nine anatomical points selected by the prosthetist, and the completion of the wing of the prosthetic socket through interpolation.

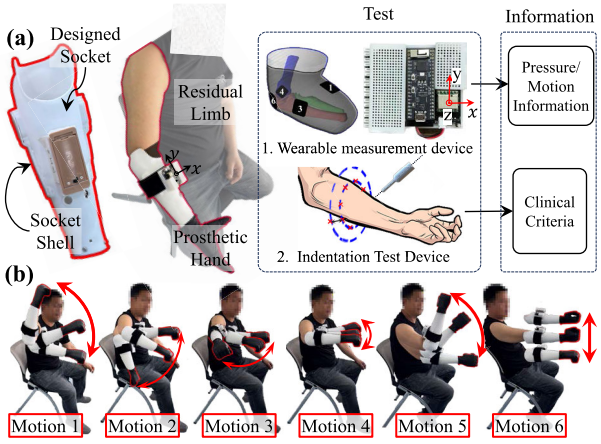

Fig. 4. Key information used for optimization. (a) The pressure/motion information and clinical criteria, obtained through a wearable measurement device and an indentation test device. (b) Six selected motions from the scale used to obtain the real pressure and motion information of each amputee.

scanning of residual limbs using 3D scanning technology [17], [24], computed tomography (CT) imaging data is used to construct the muscular and skeletal structures of the residual limb. This approach, based on medical imaging [25], [26], is adopted because prosthetists require anatomical details of both bones and muscles to design a well-matched socket, which simple 3D surface scanning cannot provide. Additionally, amputation surgery may make it challenging to identify anatomical regions based solely on the surface of the residual limb.

CT image data are acquired using a Siemens CT scanner (DEFINITION AS, SIEMENS, German) with a specified slice thickness of 1 mm. The data processing is conducted using MATLAB (The MathWorks Inc., USA) and Gibbon [27], a well-established tool in the field of medical image processing. Through the processing and segmentation of axial slices, a one-to-one scale structural model of the residual limb is generated (see Fig. 5), which encompasses the structures of the ulna, radius, humerus, and skin.

2) Structure Generation Based on Anatomical Positions: According to the recommendations provided by the prosthetist, the strathclyde supra olecranon socket (SSOS) was selected for fabricating sockets for the amputees [2], [28]. This method was chosen for its ability to create wings that securely encase the epicondyles, ensuring rotational stability and delivering secondary suspension. Nine anatomical points (see Fig. 3) are delineated by the prosthetist, which includes p1 (located at the humerus, specifically the coronoid fossa), p2 (situated at the ulna, along the shaft's interior edge), p3 (found at the radius, along the shaft's lateral edge), p4 (positioned at the humerus, at the medial epicondyle), p5 (marked on the upper arm's interior edge), p6 (located at the humerus, along the shaft's interior edge), p7 (situated at the humerus, along the shaft's lateral edge), p8 (identified at the humerus, specifically the lateral epicondyle), and p9 (situated on the upper arm's lateral edge).

Further, as depicted in Figure 3, these annotated points are utilized to create a curve representing the socket wing. This curve of the socket wing is generated based on a piecewise cubic Hermite interpolating polynomial, a method that is extensively employed in the field of curve design. Finally, the creation of a socket shell guided by the prosthetists is completed (see Fig. 4(a)).

B. Multi-Source Information Acquisition for Optimization

Multi-source information acquisition, which is utilized for the optimization design of the prosthetic socket, includes two

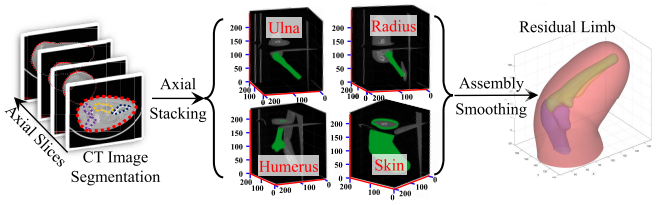

Fig. 5. The residual limb reconstruction was achieved through sequential axial superimposition and reconstruction of CT data from multiple bones and skin, followed by assembly and overall filtering.

parts: 1) the acquisition of pressure/ motion information and 2) the acquisition of clinical criteria.

1) Acquisition of Pressure/ Motion Information: A wear test was conducted to acquire pressure and motion information under six test motions (see Fig. 4(b)) selected from the ACMC scale, including

(1) Shoulder joint rotation (Motions 1 and 2).
(2) Elbow joint flexion and extension (Motions 3, 4, and 5).
(3) Forearm pronation and supination (Motion 6).

This test utilized a wearable testing device developed by our research team [3], which facilitates these data collection processes. Pressure data from six anatomical positions (see Fig. 2(a)), including the Antecubital Channel (AC), two epicondylar region contours (ERC): Lateral Epicondylar Region Contour (LC) and Medial Epicondylar Region Contour (MC), one Olecranon Region Contour (OC), and two flexor/extensor regions: Lateral Flexor/Extensor Region (LR) and Medial Flexor/Extensor Region (MR), alongside orientation data from the forearm, are both collected synchronously.

2) Acquisition of Clinical Criteria: Considering the significant variations in the mechanical properties of soft tissues from anatomical positions [29], the relationship between pressure and deformation, as well as the pain tolerance and threshold, are measured using an indentation device [30] through the indentation test. This method is commonly employed for assessing soft tissue in medicine [31] and has, in recent years, been utilized to aid in prosthetic design [9].

As illustrated in Fig. 2(b), the indentation test is conducted by applying loading and unloading at a rate of 0.2 mm/s. The relationship between pressure and deformation is continuously and automatically recorded. Meanwhile, a nearby physician promptly records the pain tolerance and threshold [32] for each anatomical site based on the patient's reports of pain perception. Three repeated measurements were taken to collect the mechanical response of pressure and deformation, as well as average pressure pain threshold and tolerance values from five subjects at six specific anatomical positions (see Fig. 2(a)).

C. Design Optimization Based on Multi-Index Info

After obtaining the multi-source information, including motion/ pressure data when wearing the prosthetic socket and clinical criteria from each amputee, such as the mechanical properties of soft tissues and pain tolerance/ threshold from anatomical positions, an optimization method will be employed to enhance the structure of the preliminary prosthetic socket. A detailed description of the proposed optimization method will be provided in Section III.

III. Optimization Method

A. Architecture of Optimization Methods

According to the Transitional Anatomically Contoured (TRAC) Interface [6] for forearm amputees, as well as insights derived from the experiences of amputees [15] and the expert design knowledge of prosthetists [16], [33], the compression length in the antecubital area and six other anatomical positions are considered pivotal in determining elbow joint mobility [12] and wearing comfort [14], respectively. Considering that minor size adjustments significantly impact the ultimate adaptability of the socket [12], based on the measured pressure and motion information, as well as the clinical criteria from each amputee, such as the mechanical properties of soft tissues and pain tolerance and threshold from anatomical positions, the optimization method for the socket design is proposed to modify compression dimensions at critical locations.

First, considering the compression length Δl of the antecubital area may affect the range of joint movement during wear, a quaternion dynamic time warping (QDTW) algorithm, which has been extensively utilized in research studies on motion similarity [34], [35], is employed to acquire the average motion similarity $\bar{r}$ under sets of wearable tests. According to the suggestion from medical professionals, $\bar{r}$ is normalized by the modification function to generate the compression length Δl of the antecubital area.

Then, the compression length Δx selected from six anatomical sites is regarded as a parameter to influence the wearing comfort in the traditional manufacturing process from prosthetists. So the average pressure $\bar{p}_{CH_i}$ from six anatomical sites acquired through specified wearable tests, as well as the measured pain pressure threshold and tolerance, compression length Δx of the mentioned anatomical sites is computed by the constructive function. Detailed descriptions of the QDTW algorithm and modification function are provided in Section III-B.

B. Multi-Index Based Structural Optimization

1) Dimension Optimization Based on Motion Information: To quantify motion similarity between the healthy limb and the residual limb equipped with a prosthetic socket, the QDTW algorithm is utilized for the analysis of two time-series orientation datasets, denoted as q_A^k and q_H^k, with lengths N and M, respectively.

$$q_A^k = \{q_{A_1}^k, q_{A_2}^k, \cdots, q_{A_n}^k, q_{A_N}^k\} \tag{1}$$

$$q_H^k = \{q_{H_1}^k, q_{H_2}^k, \cdots, q_{H_m}^k, q_{H_M}^k\} \tag{2}$$

where, $q_{A_n}^k$ and $q_{H_m}^k$ are unit quaternion type data, k corresponds to the number of selected motion tests and $k \in [1, 6]$.

A matrix T of size n-by-m is constructed to align two time-series data, where each element of the matrix is defined as follows:

$$Q_{i,j} = \left\| q_{A_i}^k - q_{H_j}^k \right\| \tag{3}$$

A warping path sequence is then constructed:

$$\psi = \{\psi_1, \psi_2, \cdots, \psi_t, \psi_T\} \tag{4}$$

here, $t \in [\max(M, N), M + N - 2]$

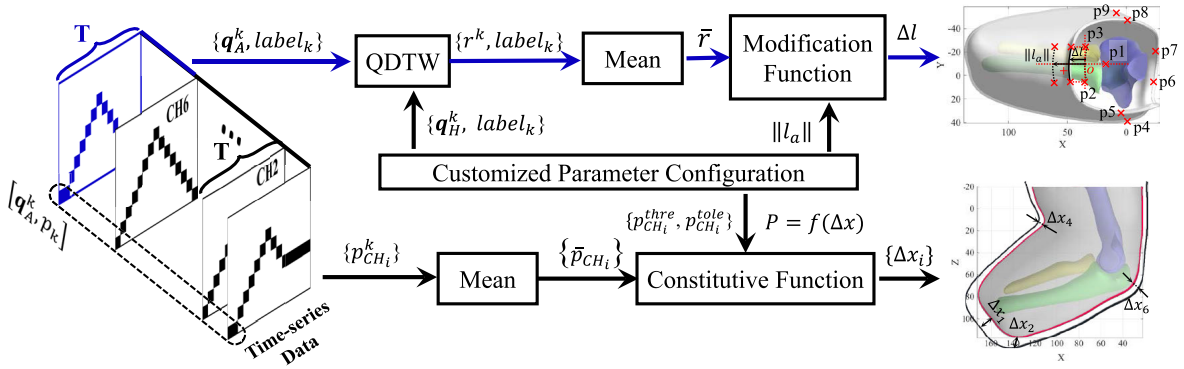

Fig. 6. Method for structural optimization of prosthetic socket utilizing time-series data, including motion data q_A^k, pressure data p_k and clinical information from six anatomical positions.

To facilitate the construction of an appropriate warping path, it is imperative that the warping path adheres to the stipulated cost function:

$$QDTW(q_A^k, q_H^k) = \arg\min \left\| \hat{\psi}_t / T \right\| \tag{5}$$

where T in the denominator is employed as a compensatory factor to account for the potential disparity in lengths among different warping path ψ, $\hat{\psi}_t = \sqrt{\sum_{t=1}^{T} \psi_t}$.

For each element of the matrix Q, the shortest distance is defined as follows:

$$\xi_{i,j} = Q_{i,j} + \min\{\xi_{i-1,j-1}, \xi_{i-1,j}, \xi_{i,j-1}\} \tag{6}$$

where, $\xi_{i-1,j-1}$, $\xi_{i-1,j}$, $\xi_{i,j-1}$ are the elements of matrix Q around $\xi_{i,j}$.

Therefore, the average motion similarity between the healthy side and the amputated side equipped with a prosthetic socket, denoted as $\bar{r}$, for two arbitrary time-series datasets subjected to the chosen motion tests of K types, can be delineated as follows:

$$\bar{r} = \frac{1}{K} \sum_{k=1}^{K} \left((\sum_{j=1}^{M} \sum_{i=1}^{N} \left\| \xi_{i,j} \right\|_k - \mu_K) / R_K \right) \tag{7}$$

where, motion type $K \triangleq 6$, $\mu_K = \frac{1}{K} \sum_{k=1}^{K} \sum_{j=1}^{M} \sum_{i=1}^{N} \left\| \xi_{i,j} \right\|_k$, $R_K = \max\{\sum_{j=1}^{M} \sum_{i=1}^{N} \left\| \xi_{i,j} \right\|_k\} - \min\{\sum_{j=1}^{M} \sum_{i=1}^{N} \left\| \xi_{i,j} \right\|_k\}$.

Based on clinical research and recommendations from medical practitioners, it can be noted that antecubital compression length Δl (refer to Figure 6) demonstrates a positive correlation with a greater degree of freedom in elbow motion. An optimized function $g(\bar{r})$ based on the sigmoid function is utilized to modify the numerical values of Δl by quantified average motion similarity $\bar{r}$.

$$\Delta l = g(\bar{r}) \cdot \|l_a\| = \left(a \cdot \frac{1}{1 + e^{-G(0.5-\bar{r})}} - b \right) \cdot \|l_a\| \tag{8}$$

here, scaling factor $a \triangleq 1.18$, $b \triangleq 0.209$, $G \triangleq 5$, Δl represents the dimension to be adjusted, while $\|l_a\|$ denotes the upper limit for compression dimensions set by a physician.

2) Dimension Optimization Based on Pressure Information and Clinical Criteria: As depicted in Figure 6, the measured pressure obtained from i regions and k types of motion tests is processed through a mean calculation to yield the average pressure, denoted as $\bar{p}_{CH_i}$, for each of the i regions.

$$\bar{p}_{CH_i} = (\sum_{k=1}^{K} p_{CH_i}^k)/K \tag{9}$$

where, $K \triangleq 6$ and represents 6 chosen motions as mentioned in Fig. 4(b).

Considering the impact of the compression length of the socket critical area on the amputees' comfort, it is necessary to adjust the compression length, denoted as Δx_i, to ensure that the pressure between the socket and the residual limb remains within the acceptable pain threshold $p_{CH_i}^{thre}$ and tolerance $p_{CH_i}^{tole}$ [32].

$$\Delta x_i = \begin{cases} f^{-1}(\bar{p}_{CH_i}) & p_1 \le \bar{p}_{CH_i} \le p_2 \\ f^{-1}(p_1) & \bar{p}_{CH_i} < p_1 \\ f^{-1}(p_2) & \bar{p}_{CH_i} > p_2 \end{cases} \tag{10}$$

where, the soft tissue response function f represents the mapping relationship between the measured deformation and pressure. A detailed description is provided in reference to Figure 8. $p_1 = \eta_l \cdot p_{CH_i}^{thre}$, $p_2 = \eta_l \cdot p_{CH_i}^{thre} + \eta_r \cdot (p_{CH_i}^{tole} - p_{CH_i}^{thre})$, $\eta_r \in [0, 1]$, $\eta_l \triangleq 1$, $i \in [1, 6]$ and represents 6 chosen areas.

3) Algorithm Process for Generating Optimized Compression Lengths: The overall optimization process for the antecubital compression length Δl and the compression lengths Δx_i of other key areas LC/MC/OC/LR/MR is shown in Algorithm 1.

IV. Experimental Protocol

A. Experimental Preparation

Five forearm amputees participated in this research with the following information: 5 males, age 46.80 ± 12.09 years, body height 1.68 ± 0.04 m, body mass 68.40 ± 4.32 kg, amputation duration 10.80 ± 8.52 years, and prosthetic limb wearing duration 9.80±9.02 years. The experimental protocol was approved by the Medical Ethics Committee of the School of Medicine, Zhejiang University (No. 2021-039). Informed

Algorithm 1 Multi-Index Based Optimization Method

Initialization:

$$\underbrace{\|l_a\|, K, T, \eta_r, \eta_l, i}_{Initial\ Para}, \underbrace{q_A^k, q_H^k}_{Motion}, \underbrace{p_{CH_i}^k}_{Pressure}, \underbrace{p_{CH_i}^{tole}, p_{CH_i}^{thre}, f(x)}_{Clinical\ Criteria}$$

Stage I: Based on QDTW

$QDTW(q_A^k, q_H^k) = \arg\min \left\| \hat{\psi}_t / T \right\|$

for k in $\{1 \ldots, K\}$ **do**

  $\bar{r} \leftarrow$ eq. 7

end for

$\Delta l \leftarrow$ eq. 8

Stage II: Based on Response Function

for k in $\{1 \ldots, K\}$ **do**

  $\bar{p}_{CH_i} \leftarrow$ eq. 9

end for

$\Delta x_i \leftarrow$ eq. 10

Ensure: Optimized compression Δx_i, Δl

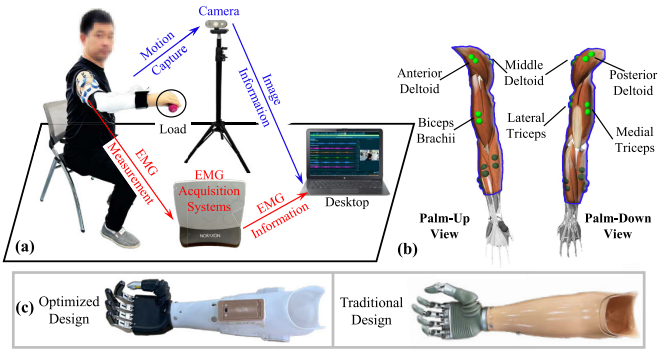

Fig. 7. The measurement equipment, measured muscle groups, and two types of prosthetic sockets used in the EMG experiment. (a): Standard EMG acquisition system and a synchronized camera were utilized for data acquisition and subsequent processing. (b): Six muscle groups were selected to evaluate adaptability improvement. (c) The optimized design and traditional design of the prosthetic sockets were employed in the experiment to compare their adaptability performance.

consent was received from all human subjects, and all the subjects depicted agreed to the use of their image.

Before the experiments, comprehensive instructions from a prosthetist with twenty years of professional experience were offered to each participant to ensure their security and precise execution of the motions in the experiments. Furthermore, the participants underwent rigorous training to familiarize themselves with these testing motions for the actual experiments.

B. Experimental Procedure

1) Indentation Test: In the indentation test, a multichannel indentation test device (see Fig. 2), which our group developed [30], and a similar device has been widely used in other studies on biomechanical properties measurement in human soft tissues [36], [37], was employed to apply loading and unloading at a rate of 0.2 mm/s (see Fig. 2(b)). A physician stationed beside promptly recorded the pain tolerance and threshold for each anatomical site in response to each patient's reports of pain perception. Three repeated measurements were conducted to obtain the mechanical response, the average values of pressure pain threshold, and tolerance [32] from five subjects at six specific anatomical positions.

2) Clinical Scale Assessment: In the second test, one type of prosthetic socket crafted using the proposed method and another type of prosthetic socket manufactured traditionally (see Fig. 7(c)) were individually donned and evaluated by each participant to assess the performance of socket adaptability. The assessment of the capacity for myoelectric control (ACMC) scale [38], a recognized standard for evaluating adaptability, was employed by a prosthetist to assess both types of prosthetic sockets under three load conditions, including a no-load condition (0 kg), a middle-load condition (0.5 kg), and a high-load condition (1 kg). Additionally, a revised version of the Trinity Amputation and Prosthesis Experience Scales (TAPES-R) was also used to evaluate amputees' subjective satisfaction with the fit and comfort of the prosthesis.

3) Fatigue Test: During the fatigue test, electromyographic (EMG) data was recorded from six muscle positions (Anterior Deltoid, Middle Deltoid, Posterior Deltoid, Biceps Brachii, Lateral Triceps, and Medial Triceps) for muscle fatigue assessment. Figure 7 illustrates the use of surface EMG sensors (Ultum EMG, Noraxon, USA), a camera (W300, HP, USA), and a PC for synchronous data recording under six test motions selected from the ACMC scale under the same three load conditions mentioned in Section IV-B.2 to complete 10 sets of repetitive motion experiments. These motions include shoulder joint rotation (Motions 1 and 2), elbow joint flexion and extension (Motions 3, 4, and 5), and forearm pronation and supination (Motion 6). The EMG sensors were secured to the subjects' skin using transparent medical tape to ensure proper contact between the electrodes (both positive, negative, and reference) and the skin. Before the experiment, all the subjects' skin was cleaned according to the guidance provided by Noraxon to ensure low impedance between the EMG sensors and the skin. The maximal voluntary contraction (MVC) of each muscle for each subject was assessed and recorded in accordance with established standard protocols [39].

4) Data Processing: The data employed for the optimization process, which encompassed motion and pressure information acquired from the wearable measurement device as well as clinical criteria (pain threshold and pain tolerance), was filtered with a low-pass Butterworth filter with a defined cut-off frequency of 50 Hz to mitigate the influence of extraneous noise disturbances. Furthermore, the EMG data, segmented under motion cycles (see Fig. 11), underwent filtration and processing to assess muscle-specific effort percentages and determine the mean frequency (MNF) and the median frequency (MDF) values across all muscles [40], [41].

In the time domain, EMG data was sequentially processed through the standard signal processing procedure [42]: filtering, rectification, and smoothing, utilizing a Finite Impulse Response (FIR) filter with specific parameters detailed in the Table I. In the frequency domain, data is processed by calculating the values of Mean Frequency (MNF) and Median Frequency (MDF) for further assessment of the fatigue level [43], [44].

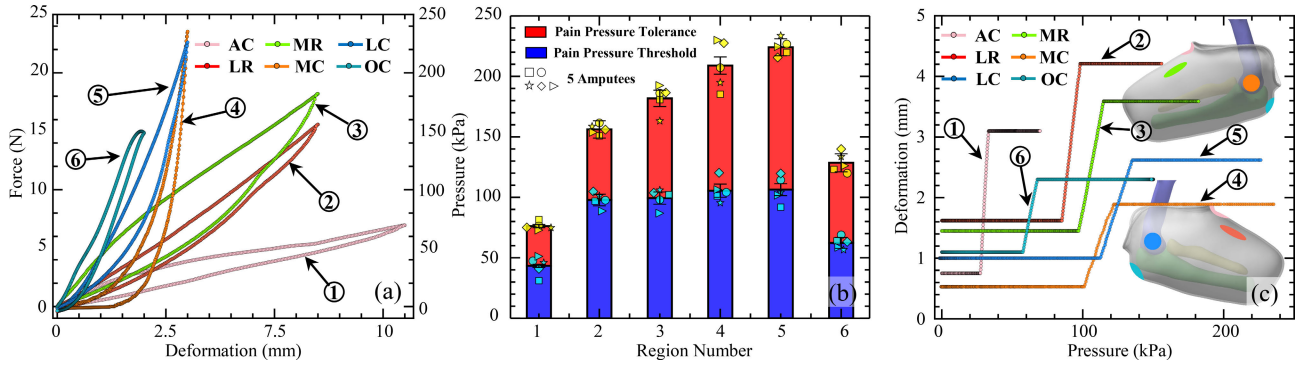

Fig. 8. Results of an indentation test and the selectable deformation values under different pressures. (a): The relationship between force and deformation for six anatomical positions. (b): Measured clinical criteria for five forearm amputees, including pain tolerance and threshold. (c): The selectable deformation value of 6 areas based on measured pressure.

TABLE I
DETAILED PARAMETERS OF SIGNAL PROCESSING METHODS

Processing Method	Type	Parameters
FIR	Bandpass	Lancosh window: 79 points, 80-250Hz
Smoothing	Mean	Window: 50 ms

V. EXPERIMENTAL RESULTS

A. Results of Indentation Test

As illustrated in Fig. 8(a), the measurement results depict noteworthy disparities in the stiffness performance of soft tissue across six distinct anatomical positions. It is of significance that the AC region is characterized by the lowest stiffness performance, whereas the OC region showcases the highest stiffness performance.

Similarly, the measurement of pain threshold and tolerance among the five amputees, as shown in Fig. 8(b), underscores substantial variability. The pain thresholds at the six anatomical positions are as follows: 42.28±1.31 kPa, 97.79±4.79 kPa, 99.35 ± 5.08 kPa, 105.49 ± 5.45 kPa, 106.34 ± 4.92 kPa, and 62.25 ± 4.54 kPa. Correspondingly, the pain tolerance at these six anatomical sites are 76.19 ± 1.31 kPa, 156.17 ± 7.17 kPa, 181.83 ± 6.71 kPa, 208.93 ± 7.15 kPa, 224.07 ± 7.02 kPa, and 128.55 ± 7.46 kPa. Notably, substantial inter-individual variations on pain tolerance are observed in the flexor/extensor region, medical epicondylar region, and olecranon region contour.

B. Results of the Optimization Parameters

The compression values of the six areas, identified by the prosthetist as key regions in the design process, are optimized based on the actual measured pressure values. The relationship between the deformation of these six areas and the actual measured pressure values is illustrated in Fig.8(c).

The optimized compression length values Δl, before the AC area for five forearm amputees are illustrated in Fig. 9. Considering the design characteristics of the strathclyde supracolecranon socket, inappropriate compression lengths may affect the elbow joint's range of motion. Thus, the initial values for each amputee were set based on the anatomical points

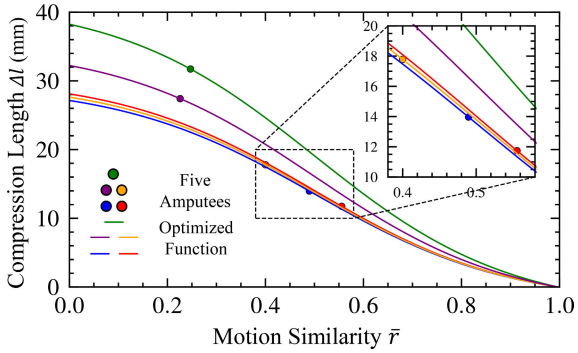

Fig. 9. Relationship between motion similarity $\bar{r}$ and compression length Δl for amputees.

(see p1, p2, p3 in Fig. 6) and the dimensions of Δl were optimized according to the measured range of motion similarity $\bar{r}$.

C. Results of the Clinical Scale Assessment

In order to further validate and compare the prosthetic socket designed by our proposed method with traditional approaches, a comparative experiment was conducted utilizing a standard ACMC scale to assess the adaptability of the two types of prosthetic sockets. Given the limitation that tests under no-load conditions may not provide a comprehensive assessment of prosthetic adaptability during actual usage, scores under three load conditions, including a no-load condition (0 kg), a middle-load condition (0.5 kg), and a high-load condition (1 kg), are depicted in Fig. 10.

The scores for five subjects under three distinct load conditions, as assessed for prosthetic sockets designed using the traditional method, are 91.83 ± 3.54, 85.09 ± 3.29, and 84.00 ± 4.64 points, respectively. Correspondingly, the scores for prosthetic sockets designed using the proposed method are 92.30 ± 1.16, 87.04 ± 1.69, and 85.75 ± 1.32 points. The traditional design method, which consists of casting, modification, and lamination processes, performed similarly to the test-wearing socket designed by the proposed method. However, when the load increases, significant differences occur between no-load and middle-load (*p< 0.05), as well as between no-load and high-load conditions (*p< 0.05). In contrast, the score of the wearing test for the socket

TABLE II
COMPARISON OF RESIDUAL LIMB MUSCLE CONDITION IN TRADITIONAL PROSTHETIC SOCKETS AND OPTIMIZED SOCKETS UNDER THREE LOAD CONDITIONS DURING FATIGUE TESTING

Load Conditon[1]	Percent Effort (%)		Mean Frequency (Hz)		Median Frequency (Hz)	
	Optimized Socket	Traditional Socket	Optimized Socket	Traditional Socket	Optimized Socket	Traditional Socket
No-Load	11.77 ± 2.41	14.20 ± 2.89	124.98 ± 5.84	119.07 ± 2.41	119.71 ± 6.99	114.35 ± 4.86
Middle-Load	13.87 ± 3.45	16.37 ± 3.13	123.24 ± 4.87	118.94 ± 6.84	119.42 ± 5.26	115.42 ± 4.39
High-Load	14.93 ± 3.93	19.22 ± 3.47	121.88 ± 3.24	115.39 ± 3.16	116.16 ± 4.27	109.45 ± 3.86

[1] The quantitative results in the table are presented as the mean value ± standard deviation.

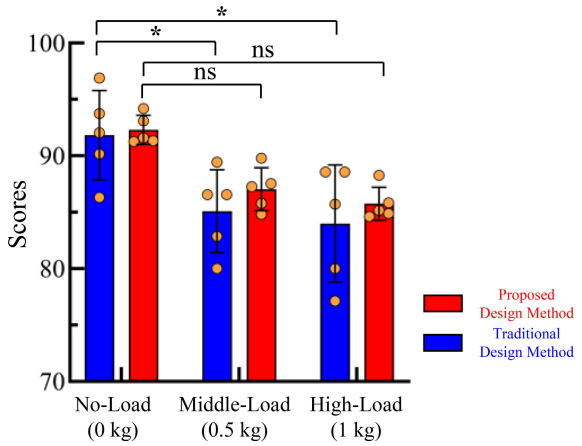

Fig. 10. A comparison between the scores obtained from the ACMC scale for the optimized prosthetic socket and the traditional prosthetic socket. Scores from the ACMC scale were acquired under three load conditions: no load, 0.5 kg load, and 1 kg load. Statistical analysis results under different load conditions have been marked (*p $<$ 0.05, where "ns" indicates no significance).

designed by the proposed method does not show significant differences between no-load and middle-load, or between no-load and high-load conditions. These results reveal that, for the score of the wearing test for the socket designed by the traditional method, these differences possibly result from the incompatibility between the residual limb and sockets, which constricts joint motion and impairs amputees' motion performance.

D. Results of Fatigue Test

Besides employing a standard ACMC scale to score and compare prosthetic limbs produced through the two methods, EMG data was utilized to analyze the subjects' percent effort across six key muscle groups under multiple load conditions and assess the level of muscle fatigue.

As depicted in Fig. 11, compared to prosthetic limbs designed by the traditional method, a notable reduction in the percent effort of these specific muscles was observed from subjects wearing prosthetic limbs designed using the proposed method. For instance, in motion 1, motion 3, and motion 6, muscle groups such as the Anterior Deltoid (AD), Biceps Brachii (BB), and Medial Triceps (MT) displayed significant decreases in percent effort. Specifically, as detailed in Table II, under the no-load condition, the average percent effort of subjects' muscle groups decreased from $14.20 \pm 2.89\%$ when wearing traditional prosthetic sockets to $11.77 \pm 2.41\%$. Similarly, under the middle-load condition, the average percent effort of subjects' muscle groups decreased from $16.37 \pm 3.13\%$ with traditional prosthetic sockets to $13.87 \pm 3.45\%$. Under the high-load condition, the average percent effort of subjects' muscle groups decreased from $19.22 \pm 3.47\%$ with traditional prosthetic sockets to $14.93 \pm 3.93\%$.

Furthermore, the MNF and MDF of the subjects' muscle groups under the three load conditions were also computed, as illustrated in Figure 12. The results indicate that the optimized prosthetic sockets, utilized under various load conditions, reduced the subjects' fatigue levels to a certain extent. Results in Table II reveal that under varying load conditions, the optimized prosthetic sockets significantly reduced subjects' muscle fatigue, as evidenced by changes in the MNF and MDF. For instance, under low-load conditions, MNF/MDF for specific muscle groups increased from 119.07 ± 2.41/ 114.35 ± 4.86 with the traditional prosthetic sockets to 124.98 ± 5.84/ 119.71 ± 6.99 with the optimized prosthetic sockets. Similar trends were observed under middle and high-load conditions, emphasizing the fatigue-reducing benefits of the optimized design.

E. Comprehensive Comparison Between Optimized and Traditional Socket Designs

A comprehensive comparison between optimized and traditional socket designs has been conducted, encompassing pressure performance under three different load conditions, clinical scale scores, and weight comparison.

As shown in Fig. 13, the satisfaction with the prosthesis section in a revised version of the Trinity Amputation and Prosthesis Experience Scales (TAPES-R) was utilized to further assess the optimized prosthetic socket from a positive evaluation perspective. The results also confirm that, from a subjective standpoint, the optimized 3D-printed prosthetic socket received higher scores (68.46 ± 3.77) compared to the traditional one (50.77 ± 6.62).

Regarding pressure, the results for different areas under three loading conditions indicate that as the test pressure increases, the advantages of the optimized prosthetic socket gradually become apparent. The traditional design process for critical dimensional adjustments of prosthetic sockets is based on amputees' subjective feedback and the prosthetist's experience. Given the muscle and nerve damage caused by amputation and individual differences in pain sensitivity, this optimization process is highly dependent on the prosthetist's expertise and the accuracy of the amputees' feedback. Additionally, it is worth noting that despite some practical grasp tests, most are conducted after the socket design is complete, neglecting the impact of the adaptability between the socket

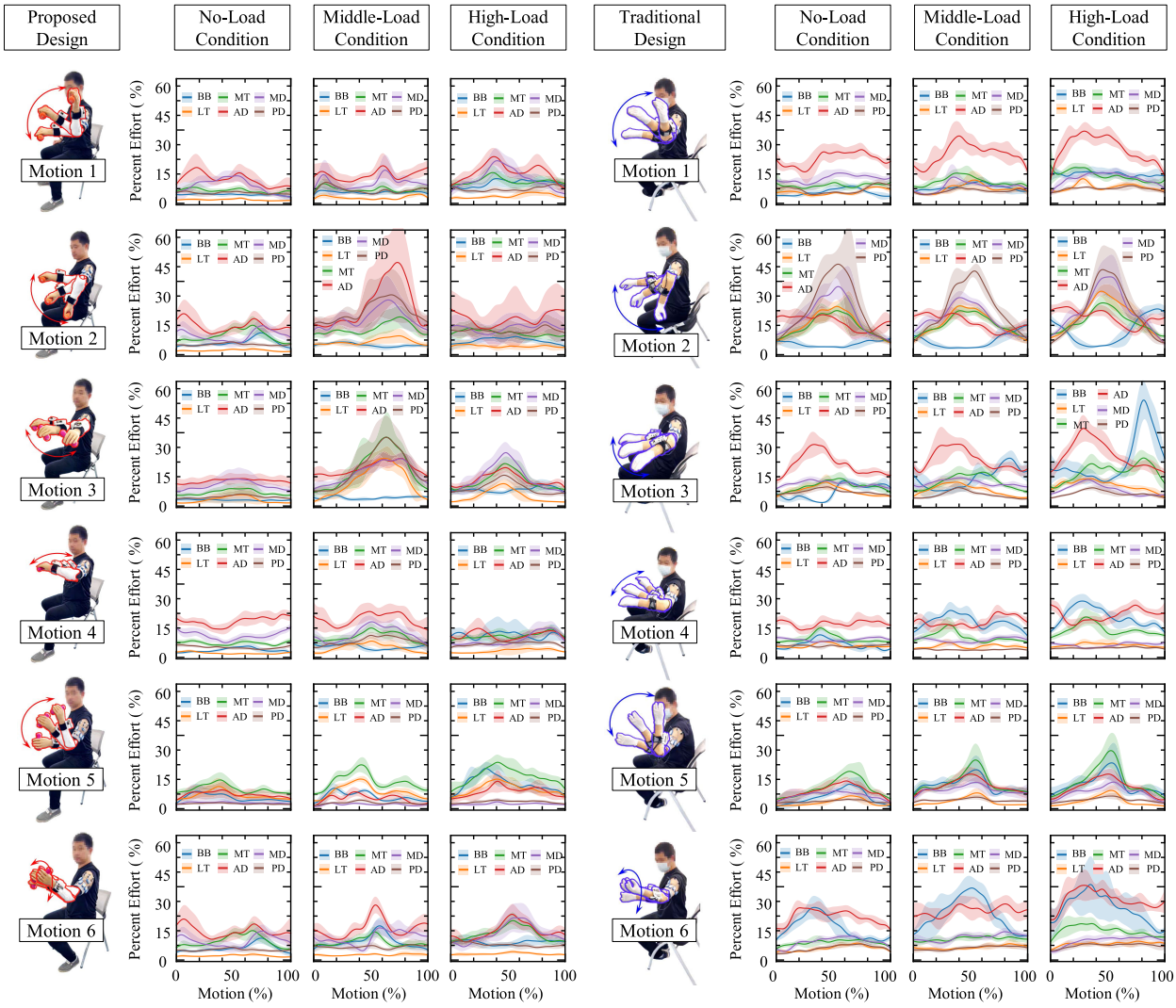

Fig. 11. The percentage effort from 5 subjects exerted by six selected muscle groups across three different loading conditions during the six sets of test motions.

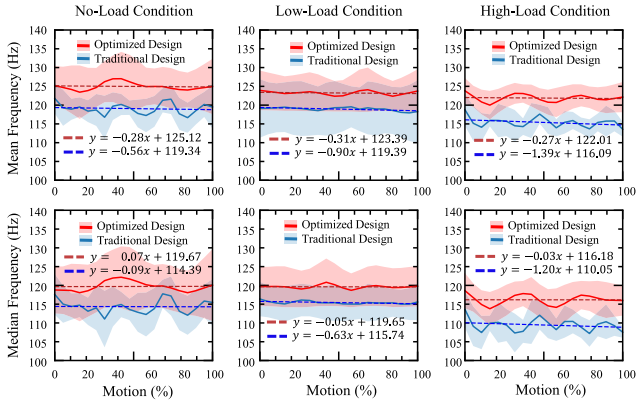

Fig. 12. An analysis of the mean and median frequency from all muscle groups when utilizing optimized prosthetic sockets versus traditional ones under three distinct loading conditions.

and the residual limb on the fluidity of actual operational movements and range of motion.

Based on feedback from amputees, it is found that weight is a particular concern for amputees. Although this weight parameter is already included in the TAPES-R scale, it is still highlighted separately in Fig. 13. The sockets manufactured using traditional methods (257.58 ± 8.99 g), which involve casting, modification, and lamination, are on average 78% heavier than those sockets (144.45 ± 8.91 g) produced using the optimized 3D printing method.

VI. Discussion

The D3Frame proposed in this paper has been presented to optimize the structural attributes of prosthetic sockets. The proposed optimization method incorporates multiple parameters, encompassing motion, pressure information, and clinical criteria, to adjust critical dimensions at key locations for the improvement of prosthetic sockets adaptability. Moreover, the prosthetists' expertise in prosthetic design is systematically quantified and implemented within the optimization approach, which includes the selection of anatomical positions and the precise adjustment of critical dimensions.

Compared with the conventional manual design approach for prosthetic sockets, as indicated in Table III, which primarily depends on the prosthetist's expertise, with the adjustment

TABLE III
RESULTS OF DIMENSIONAL ADJUSTMENT USING TWO METHODS WITHIN KEY DESIGN REGIONS

	Dimensional Adjustments within the Key Design Region (mm) [1]						
	No.1	No.2	No.3	No.4	No.5	No.6	No.7
Traditional Method	Based on the prosthetist's expertise, approximately from 0 to 6 mm.					about 0∼3	about 0∼40
Proposed Method	2.46 ±1.40	3.07 ±1.14	2.52 ±1.07	1.22 ±0.67	1.81 ±0.81	1.70 ±0.61	20.53 ±7.75

[1] The dimensions of regions No. 1 to 5 represent the compression values, while the dimensions of regions No. 6 and No. 7 represent the expansion values. Region No. 7's adjustment dimension represents the antecubital compression length, as defined in Equation 8. The adjustment dimensions in the table represent the mean± the standard deviation (std).

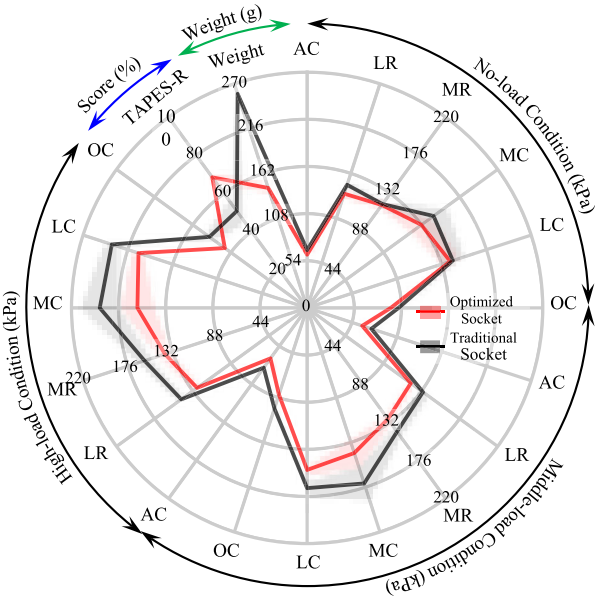

Fig. 13. An analysis of the mean and median frequency from all muscle groups when utilizing optimized prosthetic sockets versus traditional ones under three distinct loading conditions.

dimensions of vital regions, such as region 1 to 5, typically within the range of 0 to 6 mm, the dimensional adjustments based on the proposed method demonstrated a noticeable disparity, quantified at 2.22±1.23 mm. Moreover, the motion ability of residual limbs and variations in the mechanical properties of soft tissues result in significant disparities in the dimension design of prosthetic sockets. The antecubital compression length Δl is selected from 0 to 40 mm based on the traditional design method, and the compression sizes in region 5 are limited to 0∼3 mm. In contrast, when employing the proposed methodology, the antecubital compression length Δl for five subjects averages 20.53±7.75 mm, with the corresponding compression size in region 5 within 1.7±0.61 mm.

To further assess the adaptability performance of the designed prosthetic socket, five forearm amputees were recruited for a fatigue test conducted under three conditions: no-load (0 kg), middle-load (0.5 kg), and high-load (1 kg). As indicated in Table II, in comparison to the traditional design approach, the average percent effort of select muscle groups from the five subjects, when equipped with the optimized prosthetic sockets, demonstrated a respective average reduction of 17%, 15%, and 22% under the three load conditions. Meanwhile, the mean frequency increased by 5%, 3%, and 5%, and correspondingly, the median frequency exhibited an increase of 5%, 3%, and 6%. It is worth noting that, when utilizing the optimized prosthetic sockets, both mean and median frequencies consistently maintained a high level, and no significant frequency attenuation was observed under the three load conditions in the experiments.

As depicted in Table IV, despite 3D printing becoming a trend in prosthetic socket manufacturing, how to adjust dimensions and achieve structural optimization remains a major concern. Existing research focuses on the following methods: relying on the subjective design experience of prosthetists, finite element-based simulations [8], or using limited measured information-based approaches [7], [9]. Compared to previous studies, the contributions of this research are summarized as follows:

1) A data-driven design framework for the structural optimization of prosthetic sockets, centered on a multi-index based method, has been proposed. The proposed multi-index based optimization method utilizes the actual motion, pressure information, and clinical criteria of each amputee to compute the motion difference between the intact and residual limbs and extract the actual soft tissue mechanical response for size optimization of seven key anatomical regions. Compared to existing studies that use simulation models and purely rely on prosthetist design experience, the comprehensive use of objectively measured information combined with the subjective design experience of prosthetists better enhances the socket's performance for different amputees and improves the fit between the prosthetic socket and the residual limb.

2) Validation tests based on both subjective and objective methods were conducted. Five amputees were recruited to compare the optimized prosthetic socket with the traditional prosthetic socket based on clinical scale scores (ACMC scale and TAPES-R scale) and EMG-based fatigue tests under three load conditions. In contrast to the limitations in the validation of previous methods, such as the absence of different load conditions and the use of few subjects [7], [8], [9], experiments in this research were conducted under three distinct load conditions for comparative analysis of the two types of prosthetic sockets in five amputees, including both traditional designed sockets and the optimized socket. The results of two clinical scales and electromyographic signals from six muscle groups validated better-wearing adaptability for optimized prosthetic sockets.

The present study is subject to some limitations. Despite the recruitment of more subjects compared to other research, constrained by limitations in time and willingness, only 5 subjects with forearm amputations were recruited and exhibited a middle-aged demographic profile (46.80 ± 12.09 years). Furthermore, while the research results confirmed the consistency of various medical scales in evaluating the adaptability of prosthetic sockets [38], [45], [46], [47], the ACMC scale was utilized in this study without additional medical scales, which included several scoring items. Additionally, due to constraints related to subjects' limited availability and their capacity to handle heavy loads, three distinct load conditions were established, with a maximum limit of 1 kg for the applied weight. Furthermore, Some of the optimized parameters were

TABLE IV
COMPARISION OF THE PROPOSED DESIGN METHOD TO IMPROVE THE ADAPTABILITY OF PROSTHETIC SOCKET WITH OTHER RESEARCH

Studies	Method	Key Index	Optimized Parameters	Key Regions	Subjects	Vertification Method	Vertification Conditon
Herr [9] et al.2013	a data-driven design method	tissue mechanical properties	structural dimension adjustment	5 regions	1 lower extremity amputee	wearing test based on pressure	under bodyweight-load condition
Górski [7] et al.2021	objective design experience	design experience	deviation of fit	None	1 forearm amputee	wearing comfort test	under no-load conditon
Theodoros [8] et al.2022	a FEA-based design method	pressure information	structural dimension adjustment	None	None	wearing test for gait analysis	under no-load conditon
This Work	a multi-index fusion method	motion-pressure information, and clinical criteria	compression/expansion length	7 regions	5 forearm amputees	ACMC scale & fatigue assessment based on EMG	three load conditions: no-load(0 kg) middle-load(0.5 kg) high-load(1 kg)

chosen based on other research and the suggestions from a single prosthetist with 20 years of experience in prosthetic socket fabrication to decide the selection and optimization of anatomical positions and points. This research aims to improve the quality of life for amputees and future work aims to further increase the number of subjects to complete the validation and improvement of the design framework. Additionally, there is a plan to open-source the algorithm and integrate related software to achieve a more automated and convenient design process.

VII. CONCLUSION

In the present study, The D3Frame was proposed for the improvement of prosthetic socket design and its adaptability. Subsequently, a multi-index based optimization method, integrating motion/pressure information and clinical criteria, was developed to optimize the compression and expansion dimensions at selected anatomical positions. Moreover, to further substantiate the improvement of prosthetic socket adaptability based on the proposed method, verification tests were conducted based on both ACMC scale and EMG assessments, and a significant improvement was observed from the experimental results. This framework is anticipated to provide valuable assistance to clinicians in their adjustments of critical anatomical dimensions, ultimately leading to enhanced adaptability of the prosthetic socket.

REFERENCES

[1] D. Z. M. Ramirez et al., "The lived experience of people with upper limb absence living in Uganda: A qualitative study," *Afr. J. Disability*, vol. 11, p. 13, May 2022. [Online]. Available: https://ajod.org/index.php/ajod/article/view/890

[2] N. Gschwend, N. H. Scheier, and A. R. Baehler, "Long-term results of the GSB III elbow arthroplasty," *J. Bone Joint Surgery*, vol. 81, no. 6, pp. 1005–1012, Nov. 1999.

[3] Y. Gu, J. Li, W. Fan, N. Zhang, X. Zhang, and T. Liu, "A wearable monitoring system and multiindex fusion approach for adaptability assessment of prosthetic hands," *IEEE Trans. Instrum. Meas.*, vol. 73, pp. 1–11, 2024.

[4] X. Wang, F. Geiger, V. Niculescu, M. Magno, and L. Benini, "Leveraging tactile sensors for low latency embedded smart hands for prosthetic and robotic applications," *IEEE Trans. Instrum. Meas.*, vol. 71, pp. 1–14, 2022.

[5] S. Salminger et al., "Current rates of prosthetic usage in upper-limb amputees—Have innovations had an impact on device acceptance?" *Disability Rehabil.*, vol. 44, no. 14, pp. 3708–3713, Jul. 2022.

[6] J. M. Miguelez, C. Lake, D. Conyers, and J. Zenie, "The transradial anatomically contoured (TRAC) interface: Design principles and methodology," *J. Prosthetics Orthotics*, vol. 15, no. 4, pp. 148–157, Oct. 2003.

[7] F. Górski, R. Wichniarek, W. Kuczko, and M. Żukowska, "Study on properties of automatically designed 3D-printed customized prosthetic sockets," *Materials*, vol. 14, no. 18, p. 5240, Sep. 2021.

[8] T. Marinopoulos, S. Li, and V. V. Silberschmidt, "AM lower-limb prosthetic socket: Using FEA for improved mechanical performance," *Mater. Today, Proc.*, vol. 70, pp. 499–503, Jan. 2022.

[9] K. M. Moerman, D. Solav, D. Sengeh, and H. Herr, "Automated and data-driven computational design of patient-specific biomechanical interfaces," *engrXiv*, Aug. 2016, doi: 10.17605/OSF.IO/G8H9N. [Online]. Available: https://engrxiv.org/g8h9n/

[10] C. Gerzina, E. Potter, A. M. Haleem, and S. Dabash, "The future of the amputees with osseointegration: A systematic review of literature," *J. Clin. Orthopaedics Trauma*, vol. 11, pp. S142–S148, Feb. 2020.

[11] J. S. Hoellwarth, K. Tetsworth, S. R. Rozbruch, M. B. Handal, A. Coughlan, and M. Al Muderis, "Osseointegration for amputees: Current implants, techniques, and future directions," *JBJS Rev.*, vol. 8, no. 3, Mar. 2020, Art. no. e0043.

[12] J. Olsen, S. Day, S. Dupan, K. Nazarpour, and M. Dyson, "3D-printing and upper-limb prosthetic sockets: Promises and pitfalls," *IEEE Trans. Neural Syst. Rehabil. Eng.*, vol. 29, pp. 527–535, 2021.

[13] A. Ballit, I. Mougharbel, H. Ghaziri, and T.-T. Dao, "Computer-aided parametric prosthetic socket design based on real-time soft tissue deformation and an inverse approach," *Vis. Comput.*, vol. 38, no. 3, pp. 919–937, Mar. 2022.

[14] K. Ghoseiri, M. Y. Rastkhadiv, and M. Allami, "Evaluation of localized pain in the transtibial residual limb," *Can. Prosthetics Orthotics J.*, vol. 1, no. 2, pp. 26–29, Dec. 2018.

[15] N. Herbert, D. Simpson, W. D. Spence, and W. Ion, "A preliminary investigation into the development of 3-D printing of prosthetic sockets," *J. Rehabil. Res. Develop.*, vol. 42, no. 2, p. 141, 2005.

[16] J. M. Zuniga et al., "Remote fitting procedures for upper limb 3D printed prostheses," *Expert Rev. Med. Devices*, vol. 16, no. 3, pp. 257–266, Mar. 2019.

[17] Y. Zhang, K. Cheng, and L. Zhang, "3D model construction system for personalized rehabilitation prosthetics based on machine vision," *Int. J. Biol. Life Sci.*, vol. 2, no. 2, pp. 1–7, Mar. 2023.

[18] M. Hofmann et al., "Clinical and maker perspectives on the design of assistive technology with rapid prototyping technologies," in *Proc. 18th Int. ACM SIGACCESS Conf. Comput. Accessibility*, Oct. 2016, pp. 251–256.

[19] L. Aflatoony and S. J. (Susan) Lee, "AT makers: A multidisciplinary approach to co-designing assistive technologies by co-optimizing expert knowledge," in *Proc. 16th Participatory Design Conf. Participation(s) Otherwise*, vol. 2, Jun. 2020, pp. 128–132.

[20] P. Mehta et al., "A novel generalized normal distribution optimizer with elite oppositional based learning for optimization of mechanical engineering problems," *Mater. Test.*, vol. 65, no. 2, pp. 210–223, Feb. 2023.

[21] B. S. Yıldız et al., "A novel hybrid arithmetic optimization algorithm for solving constrained optimization problems," *Knowl.-Based Syst.*, vol. 271, Jul. 2023, Art. no. 110554. [Online]. Available: https://www.sciencedirect.com/science/article/pii/S0950705123003040

[22] A. Petron, J.-F. Duval, and H. Herr, "Multi-indenter device for in vivo biomechanical tissue measurement," *IEEE Trans. Neural Syst. Rehabil. Eng.*, vol. 25, no. 5, pp. 426–435, May 2017.

[23] B. J. Ranger, M. Feigin, X. Zhang, K. M. Moerman, H. Herr, and B. W. Anthony, "3D ultrasound imaging of residual limbs with camera-based motion compensation," *IEEE Trans. Neural Syst. Rehabil. Eng.*, vol. 27, no. 2, pp. 207–217, Feb. 2019.

[24] A. S. Dickinson et al., "Selecting appropriate 3D scanning technologies for prosthetic socket design and transtibial residual limb shape characterization," *JPO J. Prosthetics Orthotics*, vol. 34, no. 1, pp. 33–43, 2022.

[25] M. S. Jamaludin, A. Hanafusa, Y. Shinichirou, Y. Agarie, H. Otsuka, and K. Ohnishi, "Development of an evaluation system for magnetic resonance imaging based three-dimensional modeling of a transfemoral prosthetic socket using finite elements," *Appl. Sci.*, vol. 9, no. 18, p. 3662, Sep. 2019.

[26] X. Zhang, J. R. Fincke, and B. W. Anthony, "Single element ultrasonic imaging of limb geometry: An in-vivo study with comparison to MRI," *Proc. SPIE*, vol. 9790, pp. 463–469, Sep. 2016.

[27] K. M Moerman, "GIBBON: The geometry and image-based bioengineering add-on," *J. Open Source Softw.*, vol. 3, no. 22, p. 506, Feb. 2018.

[28] A. J. Drew, "Humerus morphology and mechanics: Informing design of a percutaneous osseointegrated docking system for above elbow amputees," Ph.D. dissertation, Dept. Biomed. Eng., Univ. Utah, Salt Lake City, UT, USA, 2018.

[29] G. Singh and A. Chanda, "Mechanical properties of whole-body soft human tissues: A review," *Biomed. Mater.*, vol. 16, no. 6, Nov. 2021, Art. no. 062004.

[30] Y. Gu, F. Meng, N. Zhang, X. Zhang, and T. Liu, "Design of a multichannel indentation system for measuring biomechanical properties of forearm soft tissues in vivo," *J. Biomechanical Sci. Eng.*, vol. 18, no. 1, 2023, Art. no. 22-00289.

[31] T. J. Hinton et al., "Three-dimensional printing of complex biological structures by freeform reversible embedding of suspended hydrogels," *Sci. Adv.*, vol. 1, no. 9, Oct. 2015, Art. no. e1500758.

[32] W. C. Lee, M. Zhang, and A. F. Mak, "Regional differences in pain threshold and tolerance of the transtibial residual limb: Including the effects of age and interface material," *Arch. Phys. Med. Rehabil.*, vol. 86, no. 4, pp. 641–649, Apr. 2005.

[33] I. Vujaklija and D. Farina, "3D printed upper limb prosthetics," *Expert Rev. Med. Devices*, vol. 15, no. 7, pp. 505–512, Jul. 2018.

[34] H. Liu, A. Panahi, D. Andrews, and A. Nelson, "An FPGA-based upper-limb rehabilitation device for gesture recognition and motion evaluation using multi-task recurrent neural networks," *IEEE Sensors J.*, vol. 22, no. 4, pp. 3605–3615, Feb. 2022.

[35] A. Mahmoud, H. Sadruddin, P. Coser, and M. Atia, "Integration of wearable sensors measurements for indoor pedestrian tracking," *IEEE Instrum. Meas. Mag.*, vol. 25, no. 1, pp. 46–54, Feb. 2022.

[36] D. Oh, S. Lee, and Y. Choi, "Simultaneous stiffness measurement device for a human forearm," *IEEE Access*, vol. 8, pp. 15313–15321, 2020.

[37] D. M. Sengeh, K. M. Moerman, A. Petron, and H. Herr, "Multi-material 3-D viscoelastic model of a transtibial residuum from in-vivo indentation and MRI data," *J. Mech. Behav. Biomed. Mater.*, vol. 59, pp. 379–392, Jun. 2016.

[38] L. M. Hermansson, A. G. Fisher, B. Bernspång, and A.-C. Eliasson, "Assessment of capacity for myoelectric control: A new rasch-built measure of prosthetic hand control," *J. Rehabil. Med.*, vol. 37, no. 3, pp. 71–166, 2005.

[39] M. Essendrop, B. Schibye, and K. Hansen, "Reliability of isometric muscle strength tests for the trunk, hands and shoulders," *Int. J. Ind. Ergonom.*, vol. 28, no. 6, pp. 379–387, Dec. 2001.

[40] A. Georgakis, L. K. Stergioulas, and G. Giakas, "Fatigue analysis of the surface EMG signal in isometric constant force contractions using the averaged instantaneous frequency," *IEEE Trans. Biomed. Eng.*, vol. 50, no. 2, pp. 262–265, Feb. 2003.

[41] J. W. Choi, C. H. Song, J. M. Kim, W. M. Jung, W. G. Kim, and H. S. Kim, "Observation of muscle activity and muscle fatigue during isotonic exercise at a constant face using metronome," *J. Biomed. Eng. Res.*, vol. 44, no. 4, pp. 284–292, 2023.

[42] A. Phinyomark, E. Campbell, and E. Scheme, "Surface electromyography (EMG) signal processing, classification, and practical considerations," in *Biomedical Signal Processing*. Singapore: Springer, 2020, pp. 3–29.

[43] A. Phinyomark, S. Thongpanja, H. Hu, P. Phukpattaranont, and C. Limsakul, "The usefulness of mean and median frequencies in electromyography analysis," in *Computational Intelligence in Electromyography Analysis—A Perspective on Current Applications and Future Challenges*, vol. 23. Rijeka, Croatia: IntechOpen, 2012, pp. 195–220.

[44] B. Elfving, G. Németh, I. Arvidsson, and M. Lamontagne, "Reliability of EMG spectral parameters in repeated measurements of back muscle fatigue," *J. Electromyogr. Kinesiol.*, vol. 9, no. 4, pp. 235–243, Aug. 1999.

[45] A. W. Heinemann, R. K. Bode, and C. O'Reilly, "Development and measurement properties of the orthotics and prosthetics users' survey (OPUS): A comprehensive set of clinical outcome instruments," *Prosthetics Orthotics Int.*, vol. 27, no. 3, pp. 191–206, 2003.

[46] C. Gummesson, I. Atroshi, and C. Ekdahl, "The disabilities of the arm, shoulder and hand (DASH) outcome questionnaire: Longitudinal construct validity and measuring self-rated health change after surgery," *BMC Musculoskeletal Disorders*, vol. 4, no. 1, pp. 1–6, Dec. 2003.

[47] P. Gallagher and M. MacLachlan, "Development and psychometric evaluation of the Trinity amputation and prosthesis experience scales (TAPES)," *Rehabil. Psychol.*, vol. 45, no. 2, pp. 130–154, 2000.